Geotechnical Engineering in the XXI Century: Lessons learned and future challenges
N.P. López-Acosta et al. (Eds.)

doi:10.3233/STAL190092

Liquefaction Analysis of Undrained Cyclic Tests by Calibration of Constitutive Models

M. GARCÍA[a,1], D. MANZANAL[b] and E. CARVAJAL-DÍAZ[a]
[a] *Keller Cimentaciones SLU, Madrid, Spain.*
[b] *Universidad Politécnica de Madrid, Spain. CONICET (Argentina)*

Abstract. Liquefaction analysis poses constitutive and numerical challenges. This work presents a calibration of constitutive models capable of reproducing liquefaction: UBC3D, Hypoplastic for sand and PM4Sand. Simulation is done with the Soil Test tool, implemented in the finite element program Plaxis, based on cyclic direct simple shear tests on Fraser River Sand. Different vertical pressures and initial densities are studied. All three models show pore pressure build-up and reach liquefaction state. In this text, some parameters are modified to accurately reproduce the experimental response. However, a unique set of parameters should be used for different applied pressures and initial densities.

Keywords. Liquefaction, cyclic tests, numerical calibration, constitutive models.

1. Introduction

Liquefaction phenomena is a challenge in geotechnical engineering due to its implications in security, especially in populated areas and key infrastructures. Liquefaction is defined as the drastic reduction of bearing capacity and stiffness of soils due to close to zero effective stresses. It is typically observed on saturated loose sands, although not restricted to these soils.

The present work is a benchmark of existing liquefaction constitutive models implemented in the commercial finite element program Plaxis. The three models analyzed and compared are: UBC3D, Hypoplastic for sand and PM4Sand.

First, shear response for undrained cyclic tests is explained, with emphasis on its dependence on initial density and applied pressure. Main characteristics of the Fraser River sand are summarized. Secondly, the formulation and parameters of the three models is summarized. Then, predictions of the models are described. Finally, some conclusions are pointed out.

2. Sand response to undrained cyclic tests

Figure 1 shows an undrained cyclic triaxial compression test on a medium dense sand. On top left is the normalized cyclic loading. Middle left figure reflects the pore-water pressure (PWP) build-up with the normalized factor r_u, which is the ratio between PWP, u, and initial applied pressure, $p_0'=p_0$. The onset of liquefaction is associated to r_u=1.0,

[1] Corresponding author; E-mail: marcos.garcia@keller.com

i.e., the pore-water pressure equals the initial applied pressure and, following the Terzaghi stress principle, effective stress is zero ($p' = p_0 - u$). Bottom left diagram presents the evolution of axial strain, which amplifies notably close to the onset of liquefaction. Top right figure displays the stress-strain response. Main features are the hysteresis due to a sharp stiffness increase at strain reversal (unloading-reloading), as well as the degradation of the stiffness modulus with increasing number of cycles. Stress path is depicted at bottom right. Confinement pressure (p') decreases as the PWP builds up and liquefaction is reached at critical state (dashed lines).

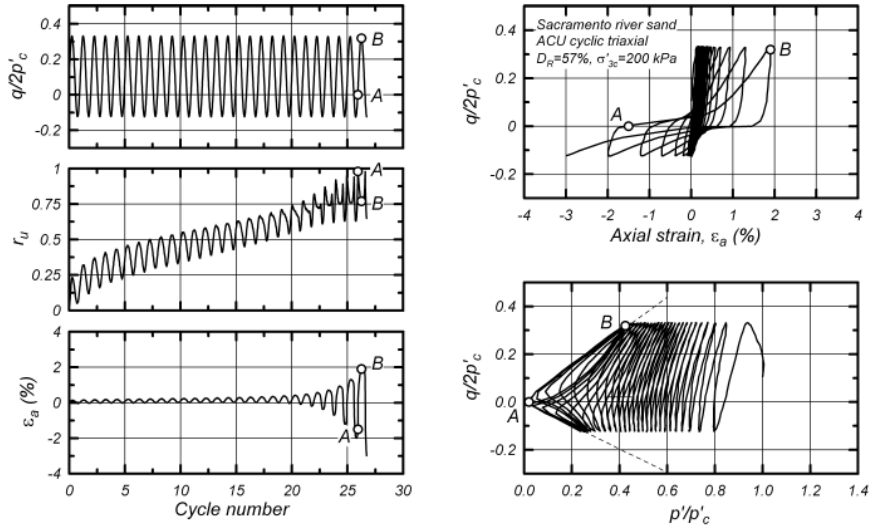

Figure 1. Medium dense sand under undrained conditions [1].

2.1. Influence of density and pressure

Liquefaction is associated to contractive behavior in drained conditions, as this is related to PWP build-up (or alternatively, effective stress reduction) in undrained conditions. Thus, the determination of contractive or dilative response of soils with respect to the critical state is a key point. Using the state parameter, ψ_s, proposed in [2]:

$$\psi_s = e - e_c \tag{1}$$

Positive values of the state parameter mean contractive response, whereas negative values mean dilative response. From Eq. (1) can be observed that void ratios (e) higher than the critical (e_c) correspond to loose contractive states while void ratios lower than the critical correspond to dense dilative states.

The critical void ratio can be expressed [3] as:

$$e_c = e_{atm} - \lambda \cdot \left(\frac{p'}{p'_{atm}} \right)^{\xi} \tag{2}$$

where p'_{atm} is the atmospheric pressure and λ and ξ are constants to be determined.

Thus:

$$\psi_s = e - e_c = e - e_{atm} + \lambda \cdot \left(\frac{p'}{p'_{atm}}\right)^{\xi} \quad (3)$$

From Eq. (2) and Eq. (3) can be seen that higher pressure produce lower critical void ratio, i.e., increases the state parameter and the soil shows an increased tendency to liquefy.

2.2. Fraser River sand and experimental program

The Cyclic simple shear tests under undrained conditions on samples of Fraser river sand are taken from the literature [4]. Characteristics of the Fraser river sand from Columbia, Canada, are listed in Table 1. From a comprehensive program available [4] some of the undrained cyclic simple shear tests are reproduced numerically (Table 2).

Table 1. Fraser river sand characteristics [4].

Parameter	Value
D_{50} (mm)	0.26
D_{10} (mm)	0.17
Cu	1.6
e_{max}	0.94
e_{min}	0.62
Gs	2.72
FC (%)	1

Table 2. Undrained cyclic shear tests on Fraser River sand [4].

Test	No.	Dr	σ'_{v0}	CSR	τ_{xy}	K_0
CDSS_40_100_12	1	40 %	100 kPa	12 %	12 kPa	0.9
CDSS_40_200_12	2	40 %	100 kPa	12 %	24 kPa	0.9
CDSS_80_100_35	3	80 %	200 kPa	35 %	35 kPa	0.9
CDSS_80_200_30	4	80 %	200 kPa	30 %	60 kPa	0.9

3. Calibration of tests with UBC3D model

3.1. Description of the model

The UBC3D model is a plasticity model initially developed by the University of British Columbia, Canada [5, 6], implemented as a 3D model in Plaxis [7, 8]. Table 3 summarizes the formulation and parameters of the model.

Table 3. UBC3D functions, formulation and parameters.

Function	Formulation	Parameter
Elastic domain	Non-linear stress dependency of stiffness Unloading elastic	K_B^e, K_G^e, me, ne
Yield surfaces	Primary (current state) and secondary (memory function)	-
Failure criteria	Mohr-Coulomb criterium	c', ϕ'_p
Hardening rule	Hyperbolic. Modified from Duncan-Chang.	K_G^p, np, Rf
Flow rule	Non-associated. Modified from Rowe	ϕ'_c
Plastic potential	Based on Drucker-Prager plastic potential.	θ=30º
Densification rule	Considers the number of cycles	n_{rev}, hard, fac_{hard}

3.2. Calibration of parameters

Table 4 lists the calibration of the parameters and the values considered. Some parameters not included are secondary ones whose values are by default. Parameters not defined as default are calibrated by trial and error.

Table 4. UBC3D parameter calibration.

Parameter	Description	Calibration	Value (default)
K_B^e, K_G^e, K_G^p (-)	Stiffness moduli[(1)]	Curve fitting	1150[(2)], 400, 450[(3)]
me, ne, np (-)	Stress-dependent exponents	Curve fitting	(0.5), (0.5), 0.4
c' (kPa)	Cohesion	CD triaxial or **DSS**	0
ϕ'_p (º)	Peak friction angle	CD triaxial or **DSS**	31.4/33.0[(4)]
ϕ'_c (º)	Critical state friction angle	CD triaxial or **DSS**	31.0
Rf (-)	Failure ratio (η_f/η_{ult}) [(5)]	Curve fitting	0.98

[(1)] e (elastic), p (plastic), B (bulk), G (shear)
[(2)] Value of 450 for tests 3 and 4
[(3)] Value of 700 for test 2
[(4)] Value 33.0 for Dr=80% (tests 3 and 4)
[(5)] η: stress ratio=q/p'

4. Calibration of tests with hypoplasticity for sand model

4.1. Description of the model

Hypoplasticity assumes an incrementally non-linear rate constitutive tensor (objective co-rotational Jaumann-Zaremba stress tensor) in which strain is not split into elastic and plastic components (4) and plasticity functions (yield, flow rule, plastic potential etc.) are not explicitly defined [9, 10].

$$\dot{T} = L{:}D + N\|D\| \tag{4}$$

where T is the stress tensor, $\dot{T}$ is the stress rate, D is the strain rate tensor; L(T, e) and N(T, e) are the constitutive tensors which depend on stress and void ratio (e). Tensors L and N as implemented in Plaxis are defined by von Wolffersdorff [11]. As failure criterion the Matsuoka-Nakai surface is adopted.

To avoid ratcheting under cyclic loading, which was a shortcoming of the initial hypoplastic model, a small strain extension called intergranular stress was developed [12]. Additional parameters m_R, m_T, R_{max}, β_r and χ are introduced.

Table 5. Hypoplasticity (sand) parameters and values [13].

Parameter	Description	Calibration	value (default)
ϕ'_c (º)	Critical state friction angle	CD triaxial compression or **DSS**	31
e_{d0}	Void ratio at maximum density	Oedometer test	0.62 (e_{min})
e_{c0}	Void ratio at critical state	Oedometer test	0.94 (e_{max})
e_{i0}	Void ratio at zero pressure	Estimation from e_{max}	1.03 ($1.1e_{c0}$)
h_s (kPa)	Granular hardness	Oedometer test	$1.10e^6$
n	Exponent for compression	From d50 and Cu or oedometer	0.19
α	Exponent for peak friction angle	From d50 and Cu or triaxial test	0.1
β	Exponent-for shear stiffness	Curve fitting (drained triaxial)	2.0
p_t	Shift of stress due to cohesion	Curve fitting	($1.10e^{-5}$)
m_R	Initial and reverse shear stiffness	Small-strains tests or curve fitting	5.0
m_T	Neutral loading stiffness	Small-strains tests or curve fitting	2.0
Rmax	Size of elastic range	Small-strains tests or curve fitting	$1.10e^{-4}$
βr, χ	Rate of stiffness degradation	Small-strains tests or curve fitting	0.5, 6.0

4.2. Calibration of parameters

Table 5 summarizes the parameters, calibration procedure [13] and default values for the hypoplastic model for sands. Parameters not defined as default are calibrated by trial and error.

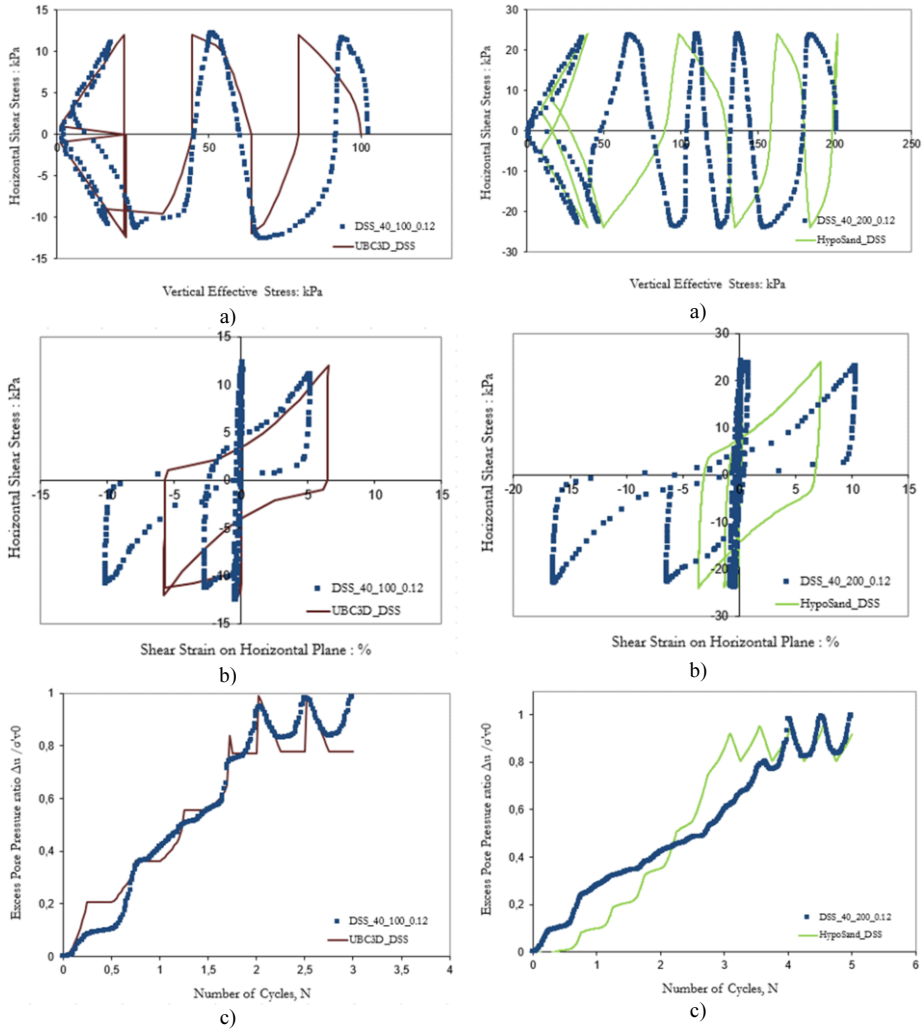

Figure 2. Test 1 (left) reproduced with UBC3D and test 2 (right) reproduced with Hypoplastic model.

5. Calibration of tests with PM4Sand model

5.1. Description of the model

PM4Sand is a plasticity model for sand under dynamic loading intended to be affordable for the design practice, as its key parameters are few and some of them are usually

available [14]. The model was developed by Boulanger and Ziotopoulou [15]. It is based on the bounding surface plasticity model for sand by Dafalias and Manzari [16]. Its key functions, formulation and parameters are listed in Table 6.

5.2. Calibration of parameters

Calibration of the model described by Vilhar [14] is followed. Parameters not defined as default are calibrated by trial and error.

Table 6. PM4Sand functions, formulation and parameters.

Function	Formulation	Parameter	Value (default)
Elastic domain	G depends on effective stress, stress ratio and fabric	G_0, ν	1000[(1)], 0.3
Yield surfaces	Small cone (stress space)	-	
Critical surface	State parameter ξ_R	ϕ'_c, D_{R0},	31, 0.4/0.8
		e_{max}, e_{min},	0.94, 0.62
		Q, R	(10), (1.5)
Bounding surface	Image back-stress ratio related to yield surface	n_b	(0.5)
Dilatancy surface	Image back-stress ratio related to yield surface	n_d	(0.1)
Hardening rule	Dilation and contraction parts are distinguished	h_{p0},	0.02[(2)]
Post-shaking	Reconsolidation due to sedimentation	PostShake	(0)

[(1)] Value of 300 for tests 1 and 2 (Dr=40%) [(2)] Value of 0.08 for tests 2

6. Performance of the models

A numerical reproduction of four undrained cyclic simple shear tests (Table 2) is performed with each of the models: UBC3D, Hypoplastic for sand and PM4Sand model. Tests are numerically simulated with the Soil Test Tool from FE program Plaxis. Performance of UBC3D and Hypoplastic models is pictured in Figure 2, and PM4Sand in Figure 3. Some of the remarkable features are:

UBC3D reproduces the PWP build-up. The unloading is elastic and the stress paths show vertical lines accordingly, which does not fit the tests. It needs different sets of parameters in some cases (Table 4).

Hypoplasticity renders an increase of pore pressure, as expected, even during unloading. Thus, stress path at liquefaction ($r_u \approx 1$) resembles the experimental one, although before reaching this state some minor differences are noticed.

A unique set of parameters are used for all four tests. However, simulation of test 1 shows a higher ratio of accumulation of pore pressure than experimentally observed. For tests 3 and 4, maximum r_u is about 85 %, but general response is predicted.

Figure 3 shows the tests 3 and 4 reproduced by the PM4Sand model. As relative density is high (80%), behavior is of cyclic mobility type. Except for the first cycles, stress path and range of variation of the excess pore pressure fits the experimental one.

All three models capture the reduction of stiffness and higher hysteresis as liquefaction advances. Some differences in the reached maximum shear strains are observed in all cases.

7. Conclusions

Some constitutive models capable of reproducing liquefaction are analyzed, namely UBC3D, Hypoplasticity for sand and PM4Sand. They capture the essential features

observed experimentally, i.e., pore water pressure build-up and associated decrease of effective stress before reaching liquefaction, as well as hysteresis and decrease of stiffness at the onset of liquefaction. Both liquefaction and cyclic mobility type behavior are reproduced. Although in this text some parameters are modified, a calibration of several tests with a unique set of parameters is the ultimate goal of constitutive models with stress and density dependence.

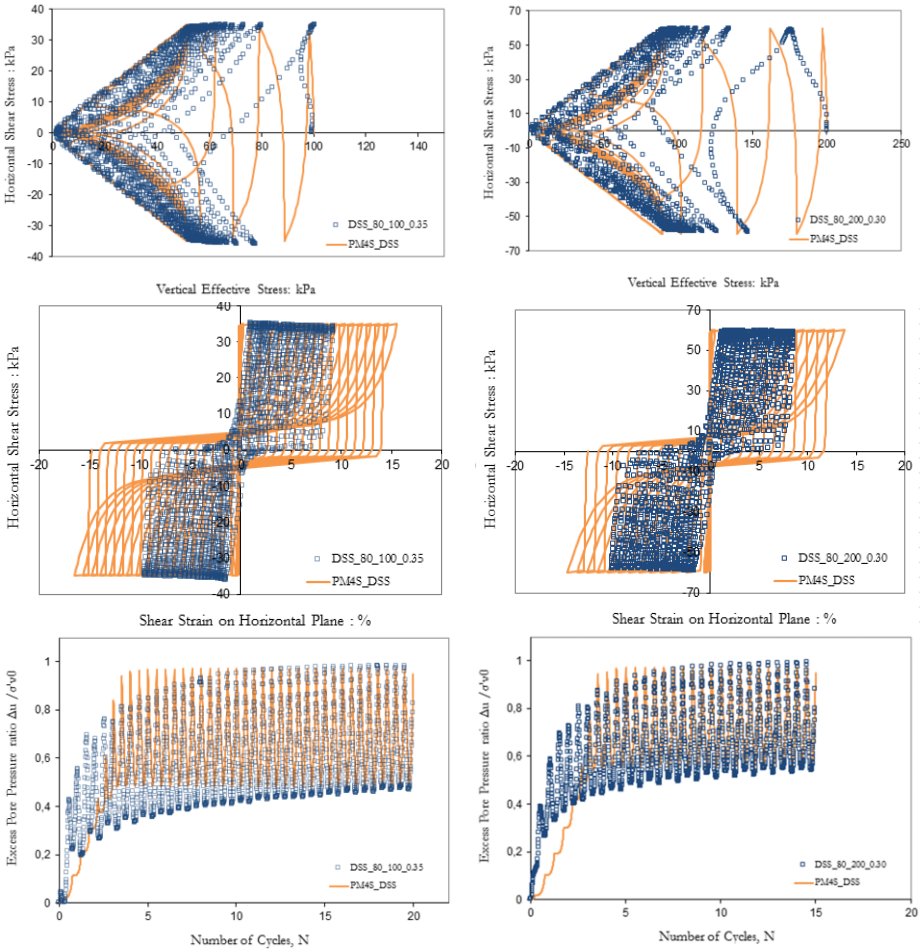

Figure 3. Test 3 (left) and test4 (right) reproduced with PM4Sand model.

Acknowledgements

Special thanks are given to Mike Jefferies and Dawn Shuttle for the processed experimental data provided.

References

[1] R. W Boulanger and S.P. Truman, Void redistribution in sand under post-earthquake loading. *Canadian Geotechnical J.* **33** (1996), 829–34.

[2] K. Been and M. Jefferies, A state parameter for sand. *Géotechnique* **35, 2** (1985), 99-102.

[3] D. Manzanal, Modelo constitutivo basado en la teoría de la plasticidad generalizada con la incorporación de parámetros de estado para arenas saturadas y no saturadas, *PhD Thesis, Universidad Politécnica de Madrid,* 2008.

[4] S. Sriskandakumar, Cyclic loading response of Fraser River sand for validation of numerical models simulating centrifuge tests, *M. Sc. Thesis, University of British Columbia,* 2004.

[5] H. Puebla, P.M. Byrne and R. Phillips, Analysis of CANLEX Liquefaction Embankments: Prototype and Centrifuge Models, *Canadian Geotechnical Journal* **34(5)** (1997), 641-657.

[6] M. Beaty and P.M. Byrne, An effective stress model for predicting liquefaction behavior of sand*, Geotechnical Earthquake Engineering and Soil Dynamics III, ASCE Geotechnical Special Publication*. **75, Vol. 1** (1998), 766-777.

[7] A. Petalas and V. Galavi, *PLAXIS Liquefaction Model : UBC3D-PLM*, PLAXIS, Delft, 2013.

[8] A. Tsegaye, Plaxis liquefaction model, *Plaxis knowledge base.* www.plaxis.com*,* 2010.

[9] G. Gudehus. A comprehensive constitutive equation for granular materials, *Soils and Foundations*, **36(1)** (1996), 1-12.

[10] D. Kolymbas, An outline of hypoplasticity, *Archive of Applied Mechanics* **61** (1991), 143-151.

[11] P.-A. von Wolffersdorff, A hypoplastic relation for granular materials with a predefined limit state surface, *Mech.cohesive-frictional mater*. **1** (1996), 251-271.

[12] A. Niemunis and I. Herle, Hypoplastic model for cohesionless soils with elastic strain range, Mech. Cohes.-Fric. Mater., **4(2)** (1997), 279–299.

[13] D. Mašín, Plaxis implementation of hypoplasticity, *Plaxis bv, Delft*, 2010.

[14] G. Vilhar, R.B.J. Brinkgreve, L. Zampich, Plaxis the PM4Sand model 2018, *Plaxis bv, Delft*, 2018.

[15] R.W. Boulanger, K. Ziotopoulou, PM4Sand (version 3.1): A sand plasticity model for earthquake engineering applications, *Report No. UCD/CGM-17/01*, (2017), 112 p.

[16] Y.F. Dafalias, M.T. Manzari, Simple plasticity sand model accounting for fabric change effects. *Journal of Engineering Mechanics* **130 (6)** (2004)**,** 622–634.